Mass fractionation of carbon and hydrogen secondary ions upon Cs^+ and O_2^+ bombardment of organic materials

Shane E. Harton[a)]
Department of Materials Science and Engineering, North Carolina State University, Raleigh, North Carolina 27695

Zhengmao Zhu and Frederick A. Stevie
Analytical Instrumentation Facility, North Carolina State University, Raleigh, North Carolina 27695

Dieter P. Griffis
Department of Materials Science and Engineering, North Carolina State University, Raleigh, North Carolina 27695 and Analytical Instrumentation Facility, North Carolina State University, Raleigh, North Carolina 27695

Harald Ade
Department of Physics, North Carolina State University, Raleigh, North Carolina 27695

(Received 17 January 2007; accepted 27 February 2007; published 2 April 2007)

A phenomenon known as mass fractionation has been probed in organic materials using secondary ion mass spectrometry (SIMS). Mass fractionation occurs because two isotopes of a particular species (i.e., identical number of protons, but different number of neutrons) do not have identical secondary ion yields in a constant chemical environment. Two primary ion probes, Cs^+ and O_2^+, have been utilized with detection of negative and positive secondary ions, respectively, using a magnetic sector mass spectrometer. These two analysis conditions have been found to yield considerably different mass fractionation effects as a result of different sputtering and ionization mechanisms. Also, as determined previously with SIMS analysis of inorganic materials, the lower molecular weight species carbon and hydrogen are particularly susceptible to mass fractionation effects. Because organic materials are primarily composed of carbon and hydrogen, and because isotopic labeling is often utilized to accurately analyze such materials, knowledge of these effects in organic materials is essential for quantitative SIMS analysis. © *2007 American Vacuum Society.*
[DOI: 10.1116/1.2718957]

I. INTRODUCTION

It has been known for half of a century that, it has been known that, upon bombardment of a material with a charged species of sufficient energy, positive and negative secondary ions are emitted from the surface.[1,2] Termed secondary ion mass spectrometry (SIMS), this technique is frequently used to chemically analyze surfaces or to depth profile material films.[3–7] However, organic materials are primarily composed of carbon and hydrogen, making it difficult to distinguish different constituent materials or compounds of complex samples.[8,9] Therefore, isotopic labeling is often employed to more accurately characterize organic materials.[10,11] Isotopic labeling has also been shown to greatly minimize matrix effects[12,13] that occur through heterogeneous interfaces,[10,11] but a phenomenon known as mass fractionation is especially prevalent in low mass secondary ions such as carbon and hydrogen.[14–18] Mass fractionation occurs because two isotopes of a particular species (i.e., identical number of protons, but different number of neutrons) do not have identical secondary ion yields in a constant chemical environment.[16–18] Because of the importance of SIMS as an analytical tool, mass fractionation of secondary ions from inorganic materials, such as metals, semiconductors, and geological materials, has been thoroughly investigated over the past three decades,[18–22] yet this phenomenon has not been thoroughly investigated for organic materials. The increased use of SIMS for high-precision characterization and analysis of organic materials has made further understanding of mass fractionation in such materials essential. Here, we investigate the sputtering of negative and positive secondary ions of carbon (^{12}C and ^{13}C) and hydrogen (^{1}H and ^{2}H) from bilayer assemblies composed of unlabeled polystyrene (hPS) and deuterium-labeled polystyrene (dPS) upon bombardment of Cs^+ and O_2^+ primary ions, respectively, using a magnetic sector mass spectrometer under steady-state dynamic conditions. Results are compared to previous experimental and theoretical results for sputtering and ionization mechanisms of positive and secondary ions from inorganic surfaces upon primary ion bombardment.

Isotopic mass fractionation can often be described mathematically using a power-law formula,[23]

$$f = \frac{\varphi_L I_H}{\varphi_H I_L} \cong \left(\frac{M_L}{M_H}\right)^{\alpha}, \tag{1}$$

where f is the secondary ion yield ratio, I_L and I_H are the relative detected intensities of the light and heavy isotopes,

[a)]Author to whom correspondence should be addressed; present address: Department of Chemical Engineering, Columbia University, New York, NY 10027; electronic mail: sh2536@columbia.edu

respectively, under identical conditions and chemical composition, φ_L and φ_H are the relative fractions of the light and heavy isotopes, respectively, in the material being analyzed, M_L and M_H are the masses of the light and heavy isotopes, respectively, and α is a parameter that is dependent on the ionization and sputtering mechanisms prevalent under the analysis conditions implemented. The isotopic mass fractionation effect is sometimes measured in terms of a fractionation factor (Φ),[15] where

$$\Phi = \frac{100}{M_H - M_L}\left(\frac{1}{f} - 1\right), \tag{2}$$

and has units of %/Da.[16–18]

Two potential sputtering and ionization mechanisms are compared to the experimental results presented here. The bond-breaking mechanism[17,18] occurs when the ionization of secondary ions is dominated by the crossover from covalent to ionic bonding before emission, while the survival probability mechanism occurs when the sputtering of secondary ions is dominated by the surface work function. Experimentally, the bond-breaking mechanism ($\alpha=1$) has been observed during the analysis of inorganic materials under O_2^+ primary ion bombardment with detection of positive secondary ions,[17,18] while the survival probability mechanism ($\alpha=0.5$) has been observed with bombardment of inorganic materials with Cs^+ and detection of negative secondary ions.[15,19] Our results are consistent with prior investigations of these two mechanisms.

II. EXPERIMENT

A. Materials and sample preparation

The organic material used in this investigation, polystyrene, is a model polymer that is completely amorphous and provides a spatially uniform sample density, a moderate glass transition temperature (100 °C) allowing quenched samples to be analyzed without cryogenic cooling, and a complete absence of any heteroatoms such as oxygen or nitrogen that could cause secondary ion yield changes.[10,11] Polystyrene is also highly hydrophobic, thereby minimizing background ^1H during SIMS analysis.[24] Analysis of deuterium-labeled PS is necessary for the investigation of hydrogen mass fractionation because the natural abundance of deuterium (^2H) is only 0.015%,[25] making accurate depth profiling of naturally occurring ^2H very difficult.[22] In contrast, ^{13}C is a relatively abundant minor isotope (1.1%).[10,11,25] Time-of-flight (ToF) SIMS was used to characterize the degree of deuterium substitution in the dPS (φ_d).[11,26] For this, Si (100)wafers were cut into 1×1 cm^2 squares, soaked in BakerClean JTB-111 (J. T. Baker) for 30 min, and then rinsed with de-ionized (DI) water. The substrates were then soaked in aqueous hydrofluoric acid (J. T. Baker, 10% v/v) for 1 min, washed with DI water, and blown dry with nitrogen. Thin (~30 nm) dPS (Polymer Source; $M_w=82.8$ kDa; $M_w/M_n=1.15$) samples were immediately prepared on the hydrogen-passivated (SiH) substrates. The dPS was dissolved in chromatography-grade (HPLC-grade) benzene (Aldrich) and cast onto the substrate. The samples were annealed at ~120 °C on a hot plate for 1 min and then washed with HPLC-grade *n*-heptane (Aldrich) and blown dry with N_2.

Bilayer assemblies of hPS on dPS were prepared for depth profiling (dynamic SIMS) using previously established procedures.[9] Silicon (100) wafers were cut into 2×2 cm^2 squares and cleaned and etched according to the procedures outlined above. The SiH substrates were either immediately cast with a polymer or placed in a UV-ozone cleaner to produce a 1.8 nm native oxide layer (SiO_x). For the bilayer preparation, a layer of dPS was cast onto SiH from toluene (Acros) to a thickness of approximately 150 nm and annealed at 140 °C for 20 min under vacuum (~10^{-3} mm Hg) to remove all residual solvent and allow the chains to relax and retain a bulk density. Next, hPS (Polymer Source; $M_w=73.0$ kDa; $M_w/M_n=1.04$) was cast onto SiO_x from toluene, scored with a sharp tip, floated into DI water, and picked up with the dPS-coated SiH substrates. The bilayer assembly was annealed at 90 °C for 12 h under vacuum, which removed residual solvent without allowing hPS/dPS interdiffusion. Finally, a 20 nm (nominal) gold coating was sputtered onto the surface of the films prior to SIMS analysis to assist in charge removal (passive charge neutralization).[9,27]

B. Time-of-flight SIMS analysis

ToF SIMS measurements were performed with a PHI TRIFT I instrument using a ^{69}Ga liquid metal ion gun at 15 kV primary high voltage and 7.5 kV extraction voltage. A potential of 3 kV was applied to the sample holder for the extraction of positive secondary ions. A pulsed $^{69}Ga^+$ primary ion beam was used to raster over 100×100 μm^2 sample surface areas. Data acquisition time was set to 7 min, resulting in a total primary ion fluence of ~5×10^{11} ions/cm^2 per analysis (static conditions).[11] Mass spectra were collected from three different spots and were subsequently analyzed using the WINCADENCE commercial software. The tropylium ion ($C_7H_7^+$) was the species used for determining φ_d, as this molecular ion has minimal mass fractionation effects among the various isotopic permutations[15,26] and negligible background interferences. The positive secondary ion mass spectrum of dPS from 96 to 99 Da is shown in Fig. 1. The peaks at 97 and 98 Da (nominal) each contain two species, which are not mass resolved (see Table I). Therefore, the known natural abundance of ^{13}C (i.e., 7.7% of the tropylium ions contain a ^{13}C)[11] was used to subtract the ^{13}C-containing variants at 97 and 98 Da. The results of this analysis are shown in Table I, with $\varphi_d=0.962$.

C. Dynamic SIMS analysis

A CAMECA IMS-6f magnetic sector mass spectrometer was used to depth profile the hPS/dPS films.[9] Two primary ion sources, Cs^+ and O_2^+, were chosen because of their common use for SIMS depth profiling of various materials. Cs^+ bombardment is known to enhance negative secondary ion yields,[2,28] while O_2^+ bombardment is known to enhance posi-

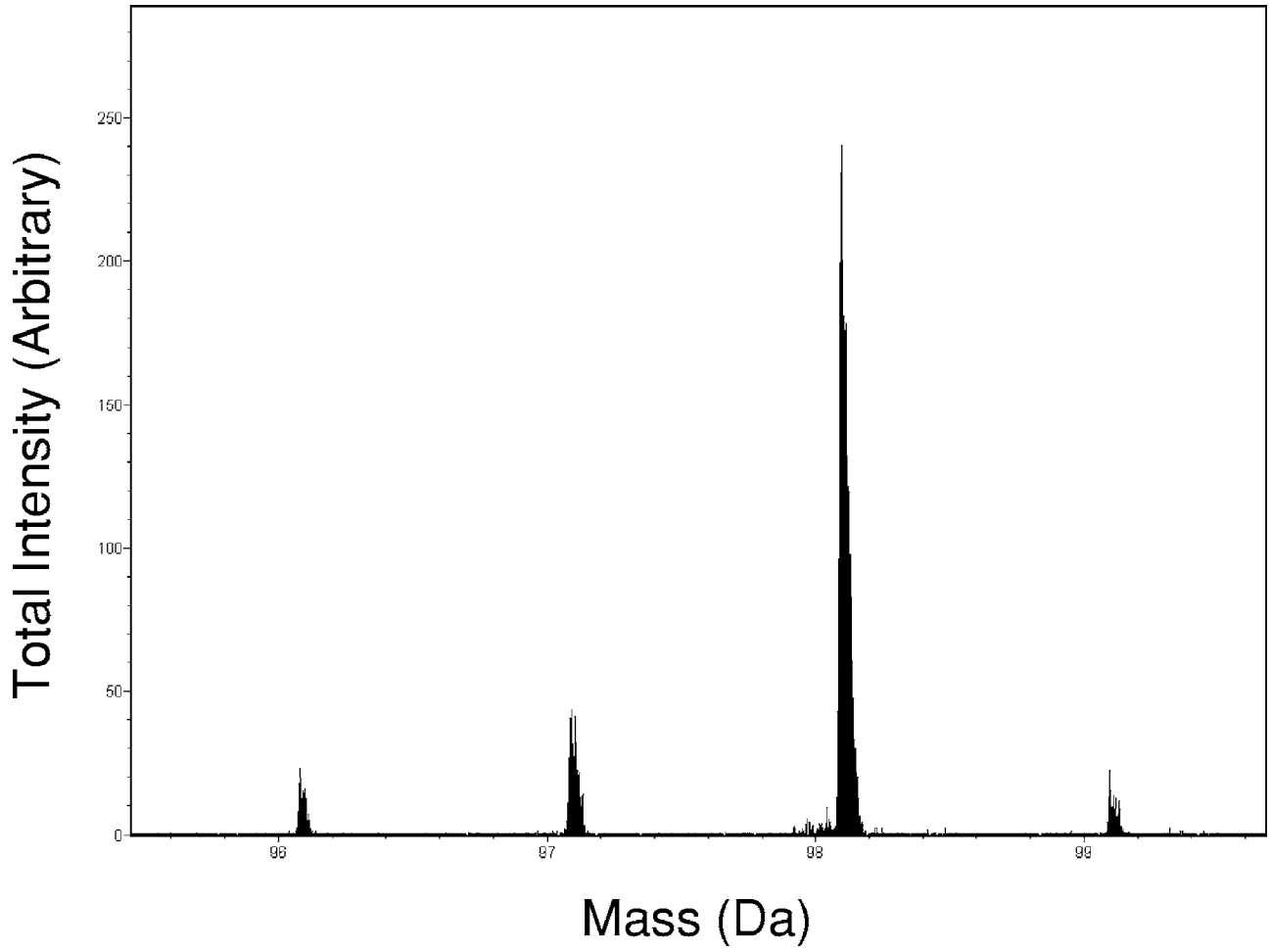

FIG. 1. Positive ion ToF SIMS spectrum (0.04 Da bin) for dPS (96–99 Da). From an average over three spectra, the degree of deuterium substitution in dPS (φ_d) was determined to be 0.962.

tive secondary ion yields.[29] Typical analysis conditions for O_2^+ primary ion bombardment included a 30 nA primary current rastered over a 180×180 μm^2 area, with 5.5 keV impact energy (10 kV primary with 4.5 kV sample bias). The angle of incidence for the primary ions was 41°. The mass resolution ($m/\Delta m$) was set to 3000 for separation of ^{13}C and $^{12}C^1H$ for carbon fractionation measurements,[10,11] while $m/\Delta m=1250$ was used to separate ^2H from $^1H_2$ for hydrogen fractionation measurements.[30,31] Positive secondary ions were detected from a 60 μm diameter optically gated area positioned in the center of the raster. As determined previously, measurable sample charging does not occur under these conditions.[31]

TABLE I. ToF SIMS results from analysis of the tropylium ion ($C_7H_7^+$) of dPS (see Fig. 1). The exact masses are reported from a database within the WINCADENCE commercial software, and the compositions are averaged over three spectra.

Species	Exact mass (Da)	% composition
$^{12}C_7{}^2H_5{}^1H_2$	96.0861	5.7±0.33
$^{13}C^{12}C_6{}^2H_5{}^1H_2$	97.0895	0.4±0.01
$^{12}C_7{}^2H_6{}^1H$	97.0924	13.5±0.33
$^{13}C^{12}C_6{}^2H_6{}^1H$	98.0958	1.0±0.03
$^{12}C_7{}^2H_7$	98.0987	73.6±0.29
$^{13}C^{12}C_6{}^2H_7$	99.1020	5.7±0.02
$^2H/(^1H+^2H)$		96.2±0.05

For Cs^+ primary ion bombardment, typical analysis conditions included a 4 nA primary current rastered over a 120×120 μm^2 area, with 6.0 keV impact energy (5 kV primary with −1 kV sample bias) and $m/\Delta m=3100$ for both carbon and hydrogen fractionation measurements.[10,11] The angle of incidence for the primary ions was 27°. Negative secondary ions were detected from a 30 μm diameter optically gated area positioned in the center of the raster. Charge neutralization was implemented for Cs^+ bombardment and detection of negative secondary ions using the so-called "electron cloud" method.[11,32] Electrons at normal incidence to the sample are provided with a potential just below that of the sample and are present just above the surface, ensuring that the electrons do not degrade the sample or interfere with secondary ion production. In this self-compensating method, any charging due to ion bombardment of the surface of the sample is compensated by electrons that are drawn from the electron cloud. For 5 kV primary ions with a −1 kV sample bias, the typical electron coverage area is approximately

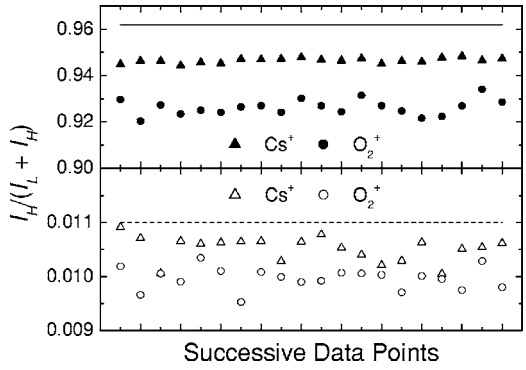

FIG. 2. SIMS reduced results $I_H/(I_H+I_L)$ for 20 consecutive data points in depth profiles obtained using 6.0 keV impact energy Cs^+ with detection of negative (▲) hydrogen and (△) carbon secondary ions and 5.5 keV impact energy O_2^+ with detection of positive (●) hydrogen and (○) carbon secondary ions. The solid and dashed lines are the actual relative fractions of ^2H and ^{13}C (φ_H) in the detected areas, respectively.

125 μm in diameter. The vacuum pressure in the CAMECA IMS-6f analysis chamber was maintained at approximately 3×10^{-10} mm Hg. The low SIMS chamber pressure, hydrophobicity of PS, and constant sputtering of the sample surface will all help to eliminate background ^1H.[33]

III. RESULTS AND DISCUSSION

The sputter rates for PS were determined, relative to (100) Si ($S_{R,PS}/S_{R,Si}$), to be 1.4 for 6.0 keV Cs^+ and 1.1 for 5.5 keV O_2^+, and the relative detected intensities for ^1H and ^{12}C (I_L) were interpolated to match the detection times of ^2H and ^{13}C (I_H), respectively. The fractionation (f) was calculated using two different statistical methods with data points within the dPS layer for the evaluation of hydrogen mass fractionation and data points within the hPS layer (>50 nm deep to avoid effects of the Au coating and the transient sputtering regime[34]) for the evaluation of carbon mass fractionation. The first statistical method used was a point-by-point calculation of f (denoted f_p) for 20 consecutive points (see Fig. 2) in one profile using Eq. (1) with $\varphi_H+\varphi_L=1$,

$$f_p=\frac{I_H}{I_L}\left(\frac{1}{\varphi_H}-1\right). \tag{3}$$

From this, averages of f_p, Φ_p [see Eq. (2)], and standard deviations thereof were determined and are shown in Table II. The values for α_p were calculated using f_p and Eq. (1).

TABLE II. Mass fractionation analysis results. f_p and Φ_p were determined from f values calculated using Eq. (3), while f_a and Φ_a were determined from f values regressed using Eq. (4). Values of α_p and α_a were determined from f_p and f_a, respectively, using Eq. (1).

	f_p	Φ_p (%/Da)	α_p	f_a	Φ_a (%/Da)	α_a
O_2^+ ($^2H/^1H$)	0.50±0.02	102±9	1.0	0.49±0.001	102±0.3	1.0
O_2^+ ($^{13}C/^{12}C$)	0.91±0.02	9.8±2	1.2	0.90±0.01	11±2	1.3
Cs^+ ($^2H/^1H$)	0.70±0.01	43±2	0.51	0.71±0.02	41±4	0.49
Cs^+ ($^{13}C/^{12}C$)	0.96±0.02	4.0±2	0.51	0.96±0.004	4.4±0.5	0.51

The second type of calculation involved a numerical minimization of the objective function (F_{obj}),[35]

$$F_{obj}=\sum_{i=1}^{20}\left(\frac{I_H(i)}{I_H(i)+f_aI_L(i)}-\varphi_H\right)^2, \tag{4}$$

which assumes a constant value of f (denoted f_a) for a given depth profile (points 1–20). The average values from two different depth profiles for f_a and Φ_a [see Eq. (2)] along with the root-mean-square differences were determined using Eq. (4). From this, α_a was determined using Eq. (1), and resulting values are shown in Table II.

The solid and dotted lines in Fig. 2 (φ_H), when compared to the measured values of $I_H/(I_H+I_L)$ for hydrogen and carbon, respectively, clearly show the effects of mass fractionation, particularly with the hydrogen isotopes. Figure 2 also shows that the analysis conditions used with Cs^+ primary ion bombardment provided an improved signal-to-noise ratio for the detection of carbon and hydrogen secondary ions when compared to the analysis conditions used with O_2^+ primary ion bombardment. Previously reported results for hydrogen mass fractionation in inorganic materials have shown $f\cong0.76$ with bombardment of Cs^+ primary ions and detection of negative secondary ions,[19] and $f\cong0.57$ with bombardment of O^- primary ions and detection of positive secondary ions.[20] This is consistent with the results shown in Table II, demonstrating that similar trends in secondary ion sputtering mechanisms are observed in organic and inorganic materials. For Cs^+ bombardment and detection of negative secondary ions, results are similar to previous observations of the survival probability mechanism ($\alpha\approx0.5$) due to a lowering of the effective surface work function upon Cs^+ implantation, which greatly increases the electron capture probability of the excited surface atoms.[15,16,19] In contrast, for O_2^+ bombardment and detection of positive secondary ions, results are similar to previous observations of the bond-breaking mechanism ($\alpha\approx1$).[14,17,18] According to this mechanism, the secondary ion yields under these conditions are governed by the production of secondary ions which involves a crossover in the nature of the bonding of the excited atoms at the surface from covalent to ionic. Mass fraction effects presented here using O_2^+ and Cs^+ bombardment with detection of positive and negative secondary ions, respectively, clearly demonstrate the importance of this phenomenon for quantitative SIMS analysis.

IV. SUMMARY AND CONCLUSIONS

Mass fractionation phenomenon has been probed for SIMS analysis of organic materials. Two types of primary ions and detection conditions were evaluated using a magnetic sector mass spectrometer under steady-state dynamic conditions. By evaluating the relative detected intensities of hydrogen (^1H and ^2H) and carbon (^{12}C and ^{13}C) isotopes, the scaling relationship in Eq. (1) was determined to be $\alpha\approx0.5$ for Cs^+ bombardment and detection of negative ions and $\alpha\approx1$ for O_2^+ bombardment and detection of positive secondary ions. This is similar to previous observations of the mass

fractionation effects in inorganic materials using similar analysis conditions.[14–19] Because of the strong influence of mass fractionation, particularly with detection of ^{1}H and ^{2}H, these results are anticipated to assist future analysis of organic materials using SIMS.

ACKNOWLEDGMENTS

This work was supported by the U.S. Department of Energy (DE-FG02-98ER45737). The authors gratefully acknowledge discussions with Prof. B. J. Garrison (The Pennsylvania State University), Prof. S. A. Schwarz (Queens College of CUNY), Dr. D. S. Simons (National Institute of Standards and Technology), and Prof. P. Williams (Arizona State University).

[1]R. E. Honig, J. Appl. Phys. **29**, 549 (1958).
[2]V. E. Krohn, J. Appl. Phys. **33**, 3523 (1962).
[3]R. E. Honig, Int. J. Mass Spectrom. Ion Process. **66**, 31 (1985).
[4]R. E. Honig, Int. J. Mass Spectrom. Ion Process. **143**, 1 (1995).
[5]A. Benninghoven, F. G. Rüdenauer, and H. W. Werner, *Secondary Ion Mass Spectrometry: Basic Concepts, Instrumental Aspects, Applications and Trends* (Wiley, New York, NY, 1987).
[6]R. G. Wilson, F. A. Stevie, and C. W. Magee, *Secondary Ion Mass Spectrometry: A Practical Handbook for Depth Profiling and Bulk Impurity Analysis* (Wiley, New York, NY, 1989).
[7]N. Winograd, Anal. Chem. **77**, 142A (2005).
[8]S. A. Schwarz *et al.*, Mol. Phys. **76**, 937 (1992).
[9]S. E. Harton, F. A. Stevie, and H. Ade, J. Vac. Sci. Technol. A **24**, 362 (2006).
[10]S. E. Harton, F. A. Stevie, and H. Ade, J. Am. Soc. Mass Spectrom. **17**, 1142 (2006).
[11]S. E. Harton, F. A. Stevie, Z. Zhu, and H. Ade, Anal. Chem. **78**, 3452 (2006).
[12]V. R. Deline, C. A. Evans, and P. Williams, Appl. Phys. Lett. **33**, 578 (1978).
[13]V. R. Deline, W. Katz, C. A. Evans, and P. Williams, Appl. Phys. Lett. **33**, 832 (1978).
[14]N. Shimizu and S. R. Hart, J. Appl. Phys. **53**, 1303 (1982).
[15]R. Middleton, D. Juenemann, and J. Klein, Nucl. Instrum. Methods Phys. Res. B **93**, 39 (1994).
[16]M. L. Yu, Phys. Rev. Lett. **40**, 574 (1978).
[17]M. L. Yu and K. Mann, Phys. Rev. Lett. **57**, 1476 (1986).
[18]G. Slodzian, J. C. Lorin, and A. Havette, J. Phys. (France) **41**, L555 (1980).
[19]P. Williams, K. M. Stika, J. A. Davies, and T. E. Jackman, Nucl. Instrum. Methods Phys. Res. **218**, 299 (1983).
[20]E. Deloule, F. Albarede, and S. M. F. Sheppard, Earth Planet. Sci. Lett. **105**, 543 (1991).
[21]A. J. Fahey and S. Messenger, Int. J. Mass. Spectrom. **208**, 227 (2001).
[22]E. Zinner, K. D. McKeegan, and R. M. Walker, Nature (London) **305**, 119 (1983).
[23]R. L. Hervig, P. Williams, R. M. Thomas, S. N. Schauer, and I. M. Steele, Int. J. Mass Spectrom. Ion Process. **120**, 45 (1992).
[24]S. Gündüz and S. Dincer, Polymer **21**, 1041 (1980).
[25]N. E. Holden, in *CRC Handbook of Chemistry and Physics*, 77th edition, edited by D. R. Lide (CRC, Boca Raton, FL, 1996), p. 11-38–11-143.
[26]S. Affrossman, M. Hartshorne, R. Jerome, H. Munro, R. A. Pethrick, S. Petitjean, and M. R. Vilar, Macromolecules **26**, 5400 (1993).
[27]A. L. Pivovarov, F. A. Stevie, and D. P. Griffis, Appl. Surf. Sci. **231–232**, 786 (2004).
[28]P. Williams, R. K. Lewis, C. A. Evans, and P. R. Hanley, Anal. Chem. **49**, 1399 (1977).
[29]A. Benninghoven, Surf. Sci. **53**, 596 (1975).
[30]S. E. Harton, F. A. Stevie, and H. Ade, Macromolecules **39**, 1639 (2006).
[31]S. E. Harton, F. A. Stevie, Z. Zhu, and H. Ade, J. Phys. Chem. B **110**, 10602 (2006).
[32]H. N. Migeon, M. Schuhmacher, and G. Slodzian, Surf. Interface Anal. **16**, 9 (1990).
[33]G. J. Clark, C. W. White, D. D. Allred, B. R. Appleton, C. W. Magee, and D. E. Carlson, Appl. Phys. Lett. **31**, 582 (1977).
[34]V. K. F. Chia, G. R. Mount, M. J. Edgell, and C. W. Magee, J. Vac. Sci. Technol. B **17**, 2345 (1999).
[35]W. H. Press, B. P. Flannery, S. A. Teukolsky, and W. T. Vetterling, *Numerical Recipes in Fortran 77: The Art of Scientific Computing*, 2nd ed. (Cambridge University Press, Cambridge, 1992), p. 387–448.